doi: 10.1017/S1431927609096561
Microsc Microanal 15(Suppl 2), 2009

In-line Holography of Embedded Nanoparticles in a TEM

Lucian Livadaru[*,**], Marek Malac[*,**], Robert A. Wolkow[*,**]

[*] National Institute for Nanotechnology, 11421 Saskatchewan Drive, Edmonton, T6G 2M9, Canada.
[**] Dept of Physics, University of Alberta, Edmonton, T6G 2G7, Canada.

Electron holography aims to retrieve the phase information about a sample, in addition to amplitude contrast. Two main setups can be used in a Transmission Electron Microscope (TEM) to acquire an in-line hologram: (A) the STEM probe mode, in which the beam crossover creates a point-source that coherently illuminates a sample, as shown in in Figure 1a [1]; and (B) the incident plane-wave setup, in Figure 1b, where the objective lens of a TEM is focused near, but not on, the sample, and a defocused image is captured which constitutes the hologram [2]. In the STEM probe setup (A) we set the imaging lens to imaging mode rather than diffraction mode (as would be the case in STEM imaging). Both setups are conceived so that at the detector plane we record the intensity of a resultant wave produced by the interference of the reference and the scattered waves. In reality, there are many such holographic setups in a TEM [3], but in this study we only concentrate on (A) and (B).

In this study we aim to (i) determine the optimal experimental parameters for in-line holograms, such as optimal defocus values for a given size of the object and sought resolution; and (ii) reduce/eliminate the twin-image problem by numerical iterative back-and-forth wavefront propagation between the planes of the true and the conjugate images. We acquire in-line holograms of our samples with a high resolution Hitachi HF3300 transmission electron microscope equipped with cold field emission source and three-lens condenser system, at electron energy of 300 kV.

In order to reconstruct an in-line hologram we adopt the Abbe imaging theory [5], according to which a reconstructed object wavefront is given to a good approximation by

$$w_{rec} = FT^{-1}\{T_z^* \cdot FT\{I_{holo}\}\} \quad (1)$$

where, T_z is the Fourier transform (FT) of the spread function, t_z at location z, and I_{holo} is the background-subtracted hologram, that is $I_{holo}(\mathbf{s}) = I_{tot}(\mathbf{s}) - A_{ref}^2(\mathbf{s})$. Generally speaking, this function is a phase-shifting factor $T_z(\mathbf{u}) = \exp[i\chi(\mathbf{u})]$, where $\mathbf{u}$ is the Fourier space vector, which includes the aberrations of the lens system. It is also known as the transfer function of the objective lens and for a given defocus value, δz, if we only consider the spherical aberration and defocus it has the following form

$$T_z(\mathbf{u}) = \exp[i\pi\lambda\delta z u^2 + i\pi C_s\lambda^3 u^4/2] \quad (2)$$

The defocus value, δz, used for a given sample size σ, a sought resolution ρ, and a detector size $N\times N$, should be optimized by accounting for the facts that (i) the hologram size acts as an aperture and thus the diffraction limit of imaging imposes $\delta z < N\rho^2/\lambda$, and (ii) The Fresnel number, $F=\pi\sigma^2/\lambda\,\delta z$, must be < 1 for the twin-image distortion to be small [4]. In addition, for crystalline samples, we have yet another defocus constraint, as we must ensure that Bragg-like fringes do not overlap with Fresnel fringes.

In order to optimize the defocus, we also carry out simulations of in-line holograms, followed by their numerical reconstruction according to the Abbe imaging theory mentioned above. In Figure 1 c and d we show simulated in-line holograms of the edge of a graphene nanoribbon obtained at two different defocus values, 1 μm and 3 μm, respectively. Note that for δz =1 μm, the

fringes of equal width in the encircled area originate from Bragg scattering, i.e. interference between scattered waves from different atoms of the sample. These fringes tamper with or destroy the reconstruction of the object wavefront. In contrast, for δz =3 μm the same area records Fresnel fringes of variable width, which are useful for rendering an accurate reconstruction of the object wavefront.

Experimental holograms of Pt/Ru nanoparticles embedded on multi-walled carbon nanotube taken at a defocus of 100 μm and nominal magnification of 120kx are shown in Figure 2a. In Figure 2b and 2c we show the amplitude reconstruction and phase reconstruction, respectively. A 3D surface plot of the phase is shown in (d), where the locations of the nanoparticles stand out as the maxima peaks of the phase map. We acknowledge NINT, NRC and NSERC for funding and thank Dr. F.Paraguay-DelGardo for kindly providing the sample.

References

[1] Gabor D., *Nature* **161**, 777-778 (1948).
[2] Volkl E., Allard L.F., and Joy D.C., Eds. *Introduction to Electron Holography.* Kluwer Academic/Plenum Publishers, New York, 1999.
[3] Cowley J.M., *Ultramicroscopy*, **41**, 335-348, 1992.
[4] Matsumoto T. et al., *Ultramicroscopy*, **54**, 317-334, 1994.
[5] Spence J.C.H. and Cowley J.M., *Principles and Theory of Electron Holography at Low Energy*, in *Introduction to Electron Holography*, Volkl E., Allard L.F., and Joy D.C., Eds. Kluwer Academic/Plenum, Publishers, New York, 1999.

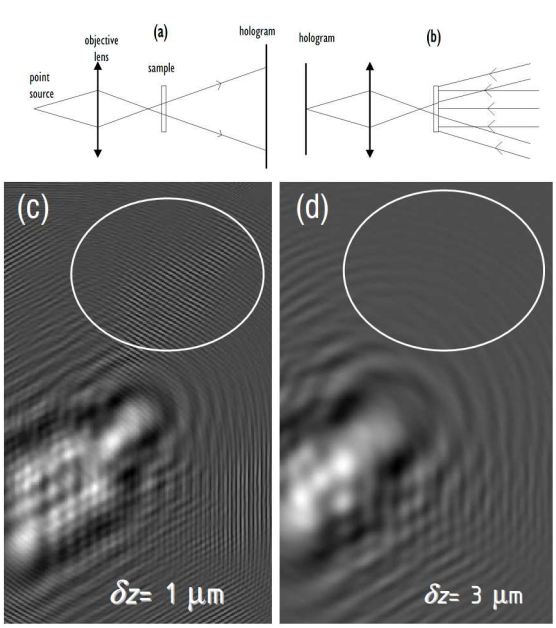

Fig 1. (a) STEM-mode in-line holographic setup featuring a point-source; (b) Incident plane-wave holographic setup used in the current study; (c,d) Simulated holograms of graphene nanoribbon for two defocus values specified on bottom; encircled regions show different types of fringes (Bragg-like in c, Fresnel-like in d) for the two cases.

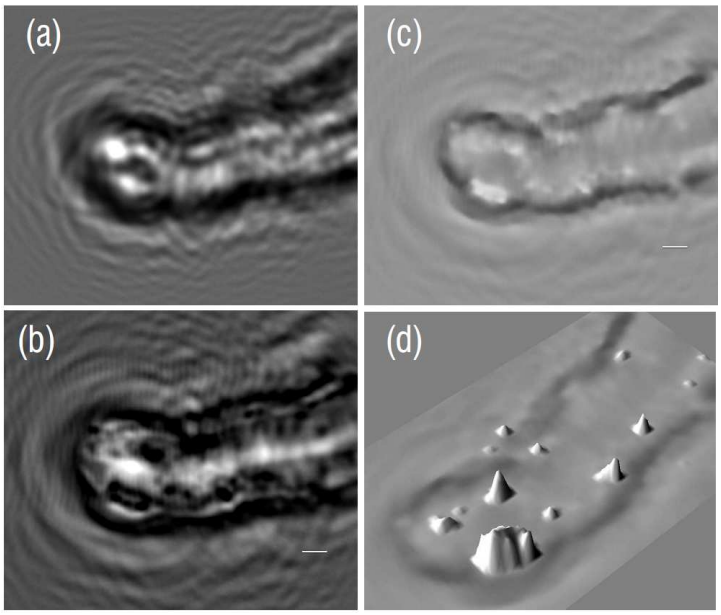

Fig 2. (a) Experimental hologram of Pt/Ru nanoparticles embedded on MWCNTs taken at a defocus value of 100 μm. (b) Amplitude reconstruction of the hologram. (c) Phase reconstruction of the hologram. The scale bars are 10 nm. (d) 3D surface plot of the phase map, emphasizing the locations of maximum phase shift at which the Pt/Ru particles are present in the sample.

https://doi.org/10.1017/S1431927609096561 Published online by Cambridge University Press